Title: Optimal features for auditory categorization

Authors: Shi Tong Liu[1], Pilar Montes-Lourido[2], Xiaoqin Wang[3], Srivatsun Sadagopan[1, 2, 4, *]

Author affiliations:

[1]Department of Bioengineering, University of Pittsburgh, Pittsburgh, PA.

[2]Department of Neurobiology, University of Pittsburgh, Pittsburgh, PA.

[3]Department of Biomedical Engineering, Johns Hopkins University, Baltimore, MD.

[4]Department of Otolaryngology, University of Pittsburgh, Pittsburgh, PA.

[*]Corresponding author.

Corresponding author:

Srivatsun Sadagopan

3501 5th Ave.,

Biomedical Science Tower 3 Room 10021

Pittsburgh, PA 15261.

Phone: (412) 624 8920

Email: vatsun@pitt.edu

Abstract

Humans and vocal animals use vocalizations (human speech or animal 'calls') to communicate with members of their species. A necessary function of auditory perception is to generalize across the high variability inherent in the production of these sounds and classify them into perceptually distinct categories (‘words’ or ‘call types’). Here, we demonstrate using an information-theoretic approach that production-invariant classification of calls can be achieved by detecting mid-level acoustic features. Starting from randomly chosen marmoset call features, we used a greedy search algorithm to determine the most informative and least redundant set of features necessary for call classification. Call classification at >95% accuracy could be accomplished using only 10 – 20 features per call type. Most importantly, predictions of the tuning properties of putative neurons selective for such features accurately matched some previously observed responses of superficial layer neurons in primary auditory cortex. Such a feature-based approach succeeded in categorizing calls of other species such as guinea pigs and macaque monkeys, and could also solve other complex classification tasks such as caller identification. Our results suggest that high-level neural representations of sounds are based on task-dependent features optimized for specific computational goals.

Human speech recognition is a highly robust behavior, showing tolerance to variations in prosody, stress, accents and pitch. For example, speech features such as formant frequencies exhibit large variations within- and between- speakers[1, 2], arising from production mechanisms (production variability). To achieve accurate speech recognition, the auditory system must generalize across these variations. This challenge is not uniquely human. Animals produce species-specific vocalizations ('calls') with large within- and between-caller variability[3], and must classify these calls into distinct categories to produce appropriate behaviors. For example, in common marmosets (*Callithrix jacchus*), a highly vocal New World primate species, critical behaviors such as finding other marmosets when isolated depend on accurate extraction of call-type and caller information[4 – 8]. Similar to human speech, marmoset call categories overlap in their long-term spectra (Fig. 1A), precluding the possibility that calls can be classified based on spectral content alone, and requiring selectivity for fine spectrotemporal features to classify calls. At the same time, marmoset calls also show considerable production variability along a variety of acoustic parameters[8]. For example, '*twitter*' calls produced by different marmosets vary in such parameters as dominant frequencies, lengths, inter-phrase intervals, and harmonic ratios (Fig. 1). Tolerance to large variations in spectrotemporal features within each call type is thus necessary to generalize across this variability. Therefore, there is a simultaneous requirement for fine and broad selectivity for production-invariant call classification. The present study explores how the auditory system resolves these conflicting requirements.

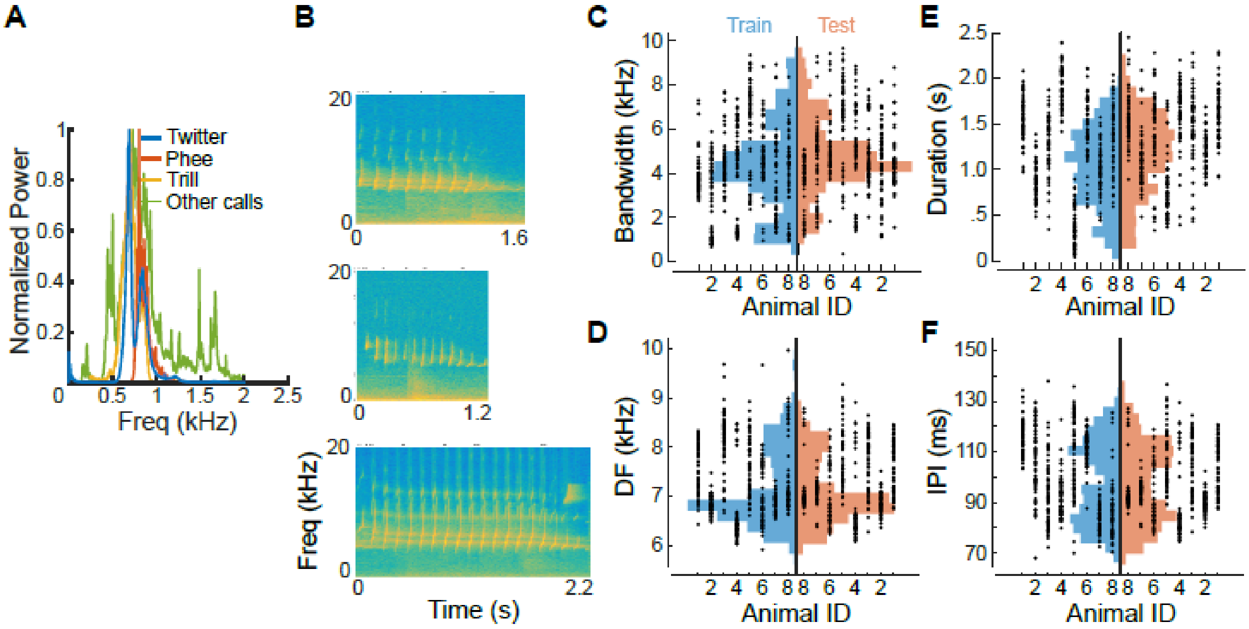

Figure 1: Production variability in marmoset calls. (A) The overall spectra of 3 major marmoset call types and other minor call types (grouped as 'Other calls'), showing spectral overlap between call categories. **(B)** Spectrograms of three twitter calls showing examples of production variability between individuals. **(C - F)** Production variability of twitter calls quantified along multiple parameters: **(C)** bandwidth, **(D)** dominant frequency, **(E)** duration, and **(F)** inter-phrase interval. Dots are parameter values of a single call produced by an individual marmoset. Histograms are overall parameter distributions, split into the training (blue) and testing (red) sets. These data show the large production variability captured by the training and test data sets, over which the model must generalize. No systematic bias is evident in calls used for model training and testing.

This problem of requiring fine- and tolerant feature tuning, necessitated by high variability amongst members belonging to a category, is not unique to the auditory domain. For example, in visual perception, object categories such as faces also possess a high degree of intrinsic variability[9 – 12]. To classify faces from other objects, using an exemplar face as a 'template' typically fails because this does not generalize across within-class variability[12]. Face detection algorithms use combinations of mid-level features, such as regions with specific contrast relationships[13, 14], or combinations of face parts[12], to accomplish classification. Of these algorithms, the one proposed by

Ullman *et al*.[12] is especially interesting because of its potential to generalize to other classification tasks across sensory modalities. In this algorithm, starting from a set of random fragments of faces, the authors used 'greedy' search to extract the most informative fragments that were highly conserved across all faces despite within-class variability. Post-hoc analyses revealed that these fragments were 'mid-level', i.e., they typically contained combinations of face parts, such as eyes and a nose. The features identified using this algorithm were consistent with some physiological observations, for example at the level of BOLD responses[15]. While the differences between visual and auditory processing are vast, these results inspired us to ask whether a similar concept – sound categorization using combinations of acoustic features – could be implemented by the auditory system.

The behavioral salience of calls for marmosets[4 – 8], and the increasing resources allocated to the processing of calls along the cortical processing hierarchy[17], suggest that call processing is a computational goal of auditory cortex. Call processing involves detecting the presence of calls in the acoustic input, classifying them into behaviorally relevant categories, extracting information about caller identity, determining the behavioral state of the caller, and developing situational awareness of the environment. Although a number of studies have described call-selective responses at various stages of the auditory pathway, there has been little investigation into how the auditory system goes about solving these problems, both at the algorithmic and mechanistic levels. In this study, we started with the premise that the detection and classification of calls into discrete call types is a critical first step that enables the above computations. Our overall question in this study was to ask how production-invariant call classification could be accomplished in the auditory pathway. Specifically, we tested the hypothesis that production-invariant call classification could be accomplished by detecting constituent features that maximally distinguish between call types. Starting from an initial set of randomly selected marmoset call features, we used a greedy search algorithm to determine the most informative and least redundant set of features necessary for call classification. We show that high classification performance can indeed be achieved by detecting combinations of a small number of mid-level features. We then demonstrate that predictions of tuning properties of putative feature-selective neurons match previous data from marmoset primary auditory cortex. Finally, we show that the same algorithm is equally successful in caller identification with marmoset calls, and in call classification in other species such as guinea pigs (*Cavia porcellus*) and macaque monkeys (*Macaca mulatta*). Taken together, our findings suggest that classification of sound categories using mid-level features may be a general auditory computation.

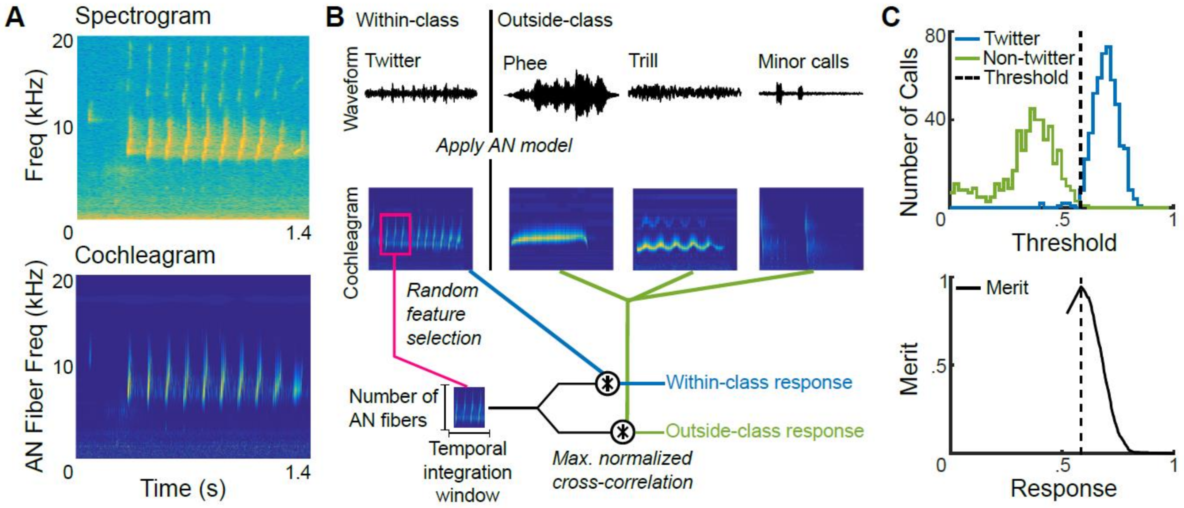

Figure 2: Initial feature generation and evaluation. (A) The spectrogram of a twitter call (top), and its corresponding cochleagram (bottom) from the application of an auditory nerve model. Color scale denotes the firing rates of auditory nerve fibers arranged by their center frequencies on the y-axis. **(B)** Schematic for initial random feature generation for a twitter (within-class) versus other calls (outside-class) categorization task. Waveforms (top) were converted to cochleagrams (middle). Random initial features were picked from twitter cochleagrams (for example, magenta box). The maximum value of the normalized cross correlation function between each call (within-class – blue, outside-class – green) and each random feature was taken to be the 'response' of a feature to a call. **(C)** Distributions (top) of a feature's responses to 500 within-class (blue) and 500 outside-class (green) calls. The mutual information (bottom) of a feature computed as a function of a parametrically varied threshold. The dotted line, corresponding to maximal mutual information, is taken to be each feature's optimal threshold. Feature 'response' has to be greater than this optimal threshold for a feature to be considered present within a call.

Results

Features of intermediate lengths and complexities are more effective for call classification

We start with the premise that the first step in call processing is the categorization of calls into discrete call types, generalizing across the production variability that is inherent to calls. Let us consider the example of classifying twitter calls from all other call types. Marmoset twitters can be characterized along several acoustic parameters such as bandwidth, duration, dominant frequency, and inter-phrase interval[8]. In Fig. 1C – F, we plot the values of these parameters for individual calls emitted by 8 animals, showing the extent of within- and between-individual variability over which generalization is required for *twitter* categorization. Similar generalization is required for categorizing the other call types as well (Supplementary Fig. 1). We first generated 6000 random initial features from the cochleagrams of 500 twitter calls emitted by 8 marmosets ('training' set, blue histograms in Fig. 1). For the purposes of this study, a 'feature' is a randomly selected rectangular segment of the cochleagram, corresponding to the spatiotemporal activity pattern of a subset of auditory nerve fibers within a specified time window. For each random feature, we determined an optimal threshold at which its utility for classifying twitters from other calls was maximized. The merit of each feature was taken to be the mutual information value at this optimal threshold in bits (Fig. 2).

In Supplementary Fig. 2, we plot the merits of all 6000 initial features as a function of each feature's bandwidth and temporal integration window. Along the margins, we plot the maximum merit of features within each bandwidth- or temporal window bin. These distributions compare the best features from each time bin, and show that features of intermediate lengths relative to the total call length show higher merits for call classification. This is an expected consequence of two characteristics of calls: 1) call types overlap in spectral content, so that brief features do not contain sufficient information to separate out categories, and 2) calls have high production variability, so that long features are less likely to be found across all calls belonging to the same category. We observed similar distributions for the classification of other marmoset call types, i.e., for trill vs. other calls, and phee vs. other calls (Suppl. Fig. 2). We characterized feature complexity using the reduced kurtosis of the activity distribution of all auditory nerve fibers contained within a feature. Briefly, if the feature was an 'empty' region of the cochleagram, or a region of uniform activity, the activity of all nerve fibers in all time bins would be about equal. This activity would thus be normally distributed, and show a reduced kurtosis value of zero. At the other extreme, for entire calls, there would be many bins of high activity, and a large number of bins with zero activity, resulting in an activity distribution with very high reduced kurtosis. We hypothesized that 'mid-level' features that represent aspects of calls such as frequency-modulated sweeps or combinations of phrases over time would show intermediate reduced kurtosis values, and be more informative than 'low-level' (tones) or 'high-level' (entire calls) features. Consistent with this idea, we found that while features of low merit showed low kurtosis values and whole calls showed high kurtosis values, features of high merit showed intermediate kurtosis values, supporting the hypothesis that 'mid-level' features of intermediate complexity were most informative for classification (Suppl.. Fig. 2).

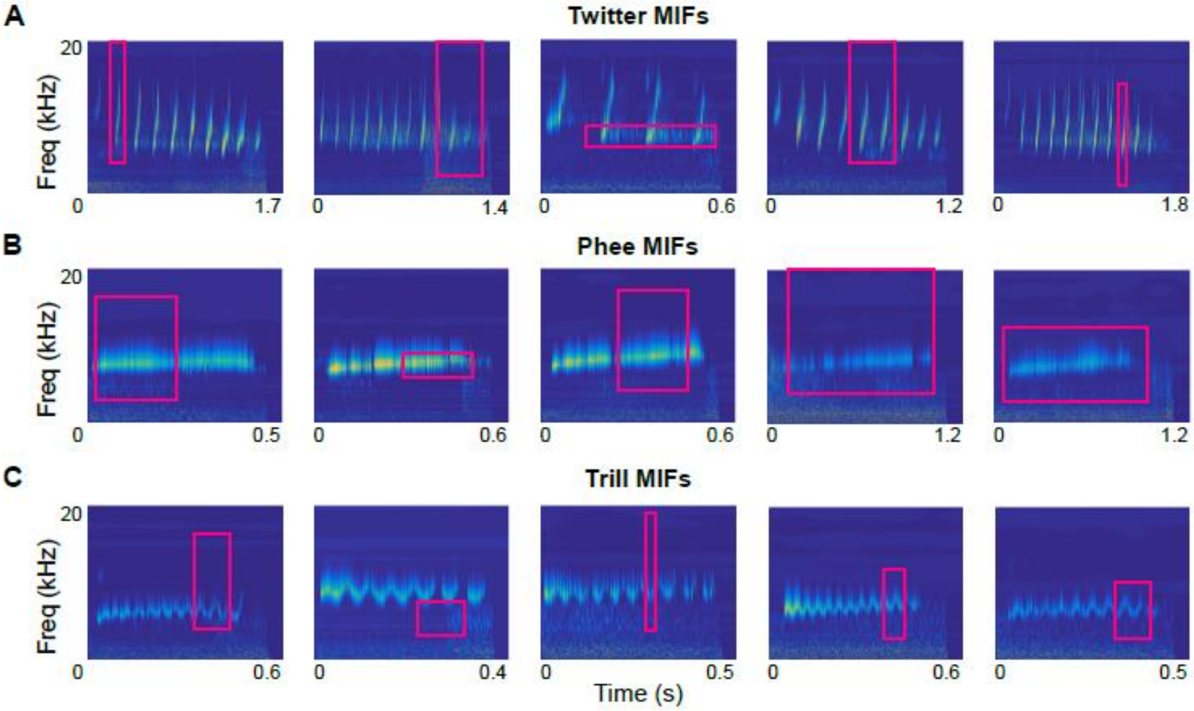

Figure 3: Most informative features for the classification of marmoset calls. Magenta boxes correspond to MIFs for the classification of twitters vs. all other calls **(A)**, phees vs. all other calls **(B)**, and trills vs. all other calls **(C)**, overlaid on the cochleagrams of the 'parent' calls from which the MIFs were obtained.

Call categorization can be accomplished using a handful of optimal features

Because we generated the initial features at random, many of these have low merit, and many are similar. Therefore, the set of optimal features for classification is expected to be much smaller than this initial set. To determine the set of optimal features that together maximize classification performance, we used a greedy-search algorithm (see Methods). Briefly, we started with the feature of highest merit, and successively added features that maximized pairwise mutual information with respect to the already chosen features. We refer to the set of these optimal features as Most Informative Features (MIFs) following the nomenclature of Ullman *et al*.[12, 18]. We determined that call classification could be accomplished using 11 MIFs for twitter vs. all other calls, 20 MIFs for trill vs. all other calls, and 16 for phee vs. all other calls. In Figure 3, magenta boxes outline the top 5 MIFs that are optimal for each of these classification tasks (the first five MIFs in Fig. 4A). The optimal features that we arrive at are mostly intuitive – for example, the top MIFs for classifying twitters detect the frequency contour of individual twitter phrases and the repetitive nature of the twitter call. In some cases, features seemed counter-intuitive – for example, the second MIF for trill classification seems to detect 'empty' regions of the cochleagram. In this theoretical framework, the lack of energy at those frequencies is also informative about the presence of a trill.

In Figure 4A, we show the pairwise information added by each MIF, the merits, and the weights of the top 10 MIFs for these classification tasks. Note that 1 bit of information corresponds to perfect classification. For twitters, detecting a single feature (the top MIF) was sufficient to gain 0.95 bits of information. Subsequent features probably detected only a few additional twitters without introducing new false alarms. For the other call types, however, the top MIF only provided 0.78 or 0.6 bits of information. Although successive MIFs individually had high merit (second column), they added little information to the top MIF (first column), likely because of redundancy – each MIF could only add a small number of additional ‘hits’ without introducing new false alarms. However, detecting these features was crucial for solving the task, as they ultimately elevated the total information to > 0.9 bits. The MIFs have positive weights, suggesting that they are informative by virtue of their presence (rather than absence) in the target category. Because we approach very high levels of classification using our pairwise optimization of mutual information, and because joint optimization of mutual information across the entire MIF set is computationally expensive, we used the pairwise-optimized MIF set for all further analyses. In frequency, MIFs neither encompassed an entire call, nor consisted of only few frequency bands. In time, MIFs showed integration windows of the order of hundreds of milliseconds (Fig. 4B). The mean MIF lengths were 215 ms, 68 ms, and 406 ms for twitters, trills, and phees respectively. Compared to the average lengths of the calls (twitters: 1.25 s, trills: 0.5 s, phees: 1.27 s), these correspond to 17%, 14%, and 32% of mean call length respectively. Interestingly, these lengths may correspond to time scales of temporal modulations in calls – for twitters, the sum of mean phrase length and mean inter-phrase interval is ~190 ms; for trills, the mean amplitude modulation period is ~30 ms. Thus, features of intermediate lengths were especially informative for call classification.

A

	Twitter			Phee			Trill		
MIF #	Added Information	Merit	Weight	Added Information	Merit	Weight	Added Information	Merit	Weight
1	0.95	0.95	14.58	0.78	0.78	10.06	0.60	0.60	7.88
2	0.01	0.84	12.14	0.01	0.67	7.76	0.10	0.12	5.37
3	0.01	0.44	9.26	0.01	0.74	8.65	0.04	0.12	4.40
4	0.01	0.85	12.49	0.01	0.71	8.29	0.04	0.25	7.13
5	0.01	0.87	12.49	0.01	0.75	8.87	0.04	0.53	7.59
6	<0.01	0.87	12.49	0.01	0.72	8.39	0.03	0.43	6.18
7	<0.01	0.80	11.71	0.01	0.71	8.27	0.03	0.29	7.44
8	<0.01	0.84	12.30	<0.01	0.71	8.27	0.03	0.27	8.14
9	<0.01	0.39	8.97	<0.01	0.75	8.90	0.02	0.27	8.26
10	<0.01	0.34	8.62	<0.01	0.71	8.49	0.02	0.22	7.74

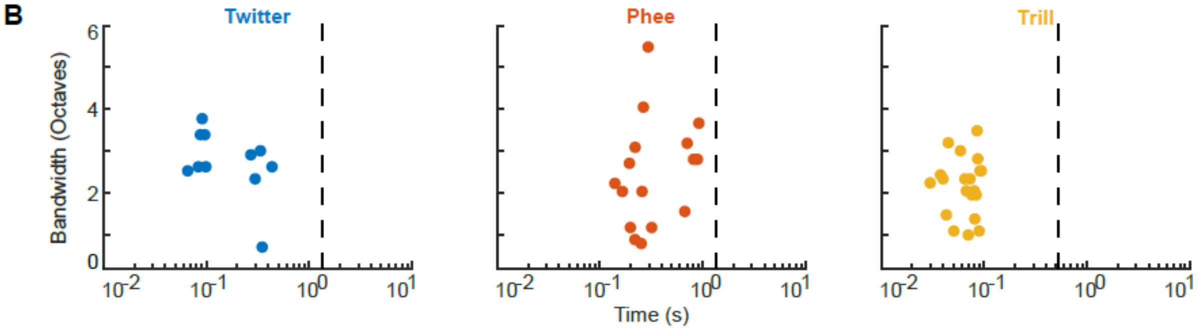

Figure 4: Information content and size of MIFs. (A) The added information, merit, and weight (log-likelihood ratio) of the top 10 MIFs for twitter, phee, and trill. **(B)** Scatter plot of the distribution of all MIFs as a function of their bandwidth and temporal integration period. Dashed line indicates the mean length of each call type.

High classification performance for novel calls can be achieved using MIFs alone

To validate our model and to test the effectiveness of using only the MIFs for classifying call types, we used a novel set of calls consisting of 500 new within-category and 500 new outside-category calls drawn from the same 8 marmosets. This ‘test’ call set did not significantly differ from the training set along any of the characterized parameters (red histograms in Fig. 1). We conceptualized each MIF as a simulated template-matching neuron whose 'response' to a stimulus was defined as the maximum value of the normalized cross-correlation (NCC) function. This simulated MIF-selective neuron 'spiked' whenever its response crossed its optimal threshold, i.e., when an MIF was detected in the stimulus. In Fig. 5, we plot the spike rasters of simulated MIF-selective neurons for twitter, phee, and trill (top 10 MIFs shown), responding to a train of randomly selected calls from the novel test set. Each spike was weighted by the log-likelihood ratio of the MIF and the weighted sum of responses in 50 ms time bins was taken as the evidence in support of the presence of a particular call type. Although occasional false positives and misses occurred, over the set of MIFs, the evidence in support of the correct call type was almost always the highest. Therefore, production-invariant call categorization is a two-step process – first, MIFs are detected in the stimuli, and then each feature is weighted by its log-likelihood ratio to provide evidence for a call type.

We quantified the performance of the entire set of MIFs (n=11, 16, and 20 for twitter, phee, and trill respectively) for the classification of novel calls by parametrically varying an overall evidence threshold and computing the hit rate (true positives) and false alarm rate (false positives) at each threshold. From these data, we plotted receiver operating characteristic (ROC) curves (Fig. 6A). In these plots, the diagonal corresponds to chance, and perfect performance corresponds to the upper left corner. The MIFs achieved >95% classification performance for all call types with very low false alarm rates.

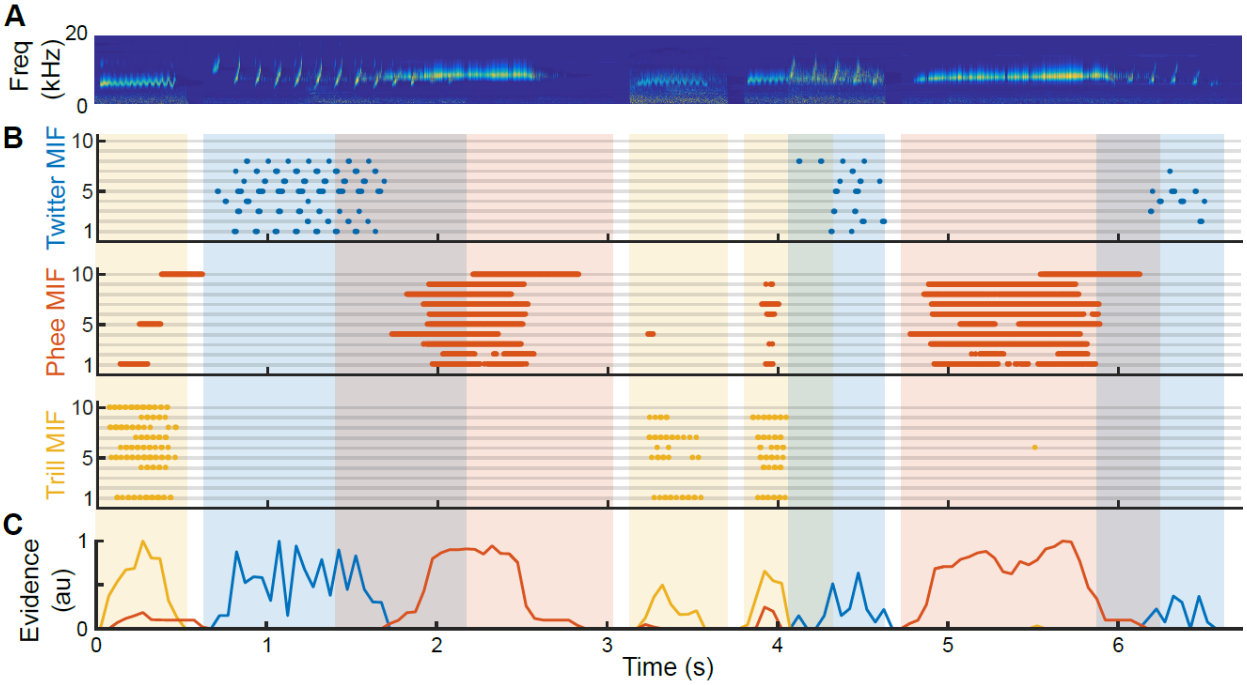

Figure 5: MIF responses to marmoset call sequences. (A) The cochleagram of a sequence of marmoset calls, some of which overlap. **(B)** Raster plot of the responses of the top 10 MIFs for twitter (top, blue), phee (middle, red), and trill (bottom, yellow). Each dot represents spiking of a putative MIF-selective neuron (i.e. when the response of the MIF exceeds its optimal threshold). **(C)** The evidence for presence of a particular call type, defined as the normalized sum of the firing rate of all MIF-selective neurons, weighted by their log-likelihood ratio. Over the duration of each call, the call type with the most evidence is considered to be present. Occasional false alarms are usually outweighed by true positive MIF detections.

Control simulations

First, we ensured that our selection of 6000 initial random features adequately sampled stimulus space. To do so, we iteratively selected sets of MIFs using our greedy search algorithm from initial random sets from which previously picked MIFs were excluded. We found that distinct sets of MIFs that had similar classification performance could be selected in successive iterations (Supplementary Fig. 3). This suggests that our initial random feature set indeed contained several redundant MIF-like features, confirming the adequacy of our initial sampling.

Second, in order to determine the contributions of various model assumptions and parameters, we repeated this process of random initial feature generation, threshold optimization, and MIF selection in different scenarios. To better visualize these differences, we used detection-error tradeoff curves (Fig. 6B), where perfect performance is the lower left corner. In this figure, the performance of the default model, as described above, is plotted in blue. First, when we used the acoustic waveform of calls instead of cochleagrams, classification performance was on average worse (Fig. 6B; red), suggesting that phase information in the waveform may be detrimental for classification. Second, we used the features with top merits without greedy-search optimization for classification, and again found that performance compared to the default model was worse (Fig. 6B, green). Finally, using entire calls as features, either treating entire individual calls as features (‘grandmother cell’ model; Fig. 6B, yellow) or using the aligned and averaged training call as a single feature (Supp. Fig. 4) also resulted in worse performance compared to the intermediate feature-based model.

We compared the cumulative information added by successive features in all of these cases using non-parametric rank-sum tests, accounting for multiple comparisons (3 comparisons) using the Bonferroni correction. In Fig. 6C, we plot the average cumulative information across all three classification tasks (twitter vs. all other calls, trill vs. all other calls, and phee vs. all other calls) for each of these conditions. The default model significantly outperformed (at $p < 0.01$) the no greedy-search model for all classification tasks. Exact p-values for the rank-sum tests, corresponding to default model comparison with the constrained model and the no-greedy-search model were: twitter (p=0.000087 and p = 0.00021, respectively), trill (p = 0.0058 and p = 0.00067, respectively), and phee (0.00015 and p = 0.00021, respectively). While the default model for trill exhibited significantly higher performance compared to the acoustic-waveform model (p = 0.000091), the default models for twitter and phee did not (p = 0.89 and p = 0.43, respectively). These results suggest that our underlying assumptions – using the cochleagram, unconstrained initial feature selection, and MIF optimization using a greedy search – were justified. Twitter MIFs were not qualitatively different when derived from calls emitted by a smaller set of animals (4 animals). Training on a set of 4 animals and testing on the other 4 animals yielded high performance (Fig. 6D), confirming the robustness of using MIFs for categorization of new calls. Twitter MIF performance in classifying twitters from other twitters was near-chance, suggesting that the estimation of mutual information values was unbiased (Fig. 6D). Finally, MIFs derived for one task (such as trill vs. other calls) showed chance level performance for other tasks (such as twitter vs. other calls; Fig. 6D), demonstrating the task-dependence of the derived MIFs.

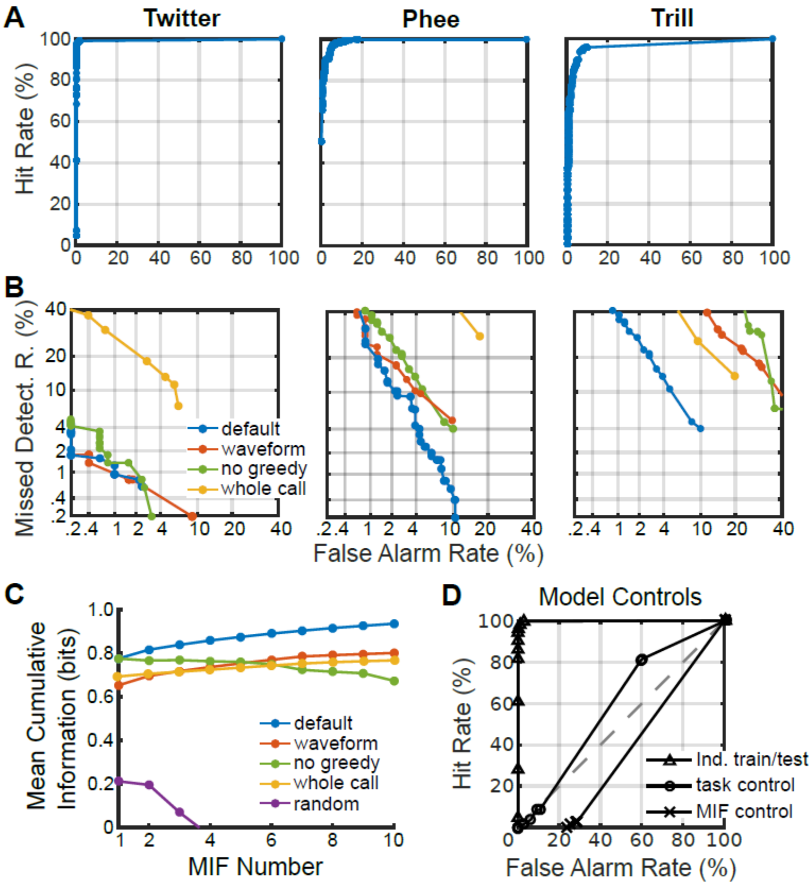

Figure 6: Classification performance and controls. (A) Receiver operating characteristic (ROC) curves for the classification of twitters, phees, and trills using MIFs alone. **(B)** Detection error tradeoff (DET) curves for comparison between classification performance of the default model (blue), and other model variations: i) MIF-based classification tested on acoustic waveforms as opposed to cochleagrams (red), ii) when features are selected without using the greedy search algorithm (green), and iii) when entire calls are used in place of features (yellow). **(C)** Comparison between various model conditions (same as B) in terms of cumulative information added by each successive feature, averaged across all three call type classification tasks. Random (purple) is the classification of twitters using randomly selected features as MIFs, averaged across 20 trials. Negative values are not shown. **(D)** ROC curves of three model controls. Independent training and testing sets (triangles) is the classification of twitters when the model is trained on the twitters of 4 animals, and tested on twitters from 4 new animals. Task control (circles) is the classification of twitters from other twitter calls, where performance is expected to be at chance levels. MIF control (crosses) is the classification of twitters using trill MIFs, also expected to be worse than chance level performance.

The precedence of intermediate-sized features for classification

We have previously shown that features of intermediate lengths and complexities possess high individual merits for classification (Supp. Fig. 2). We have also shown that the set of MIFs is composed mainly of features of intermediate lengths relative to the entire call (Fig. 4B). To directly test whether features of intermediate size were indeed the most informative, we re-derived MIFs after constraining the initial set of features to particular time and frequency bins and quantified model performance (Fig. 7). When we constrained the features to be only small (<100 ms and <1 oct.) or removed all small features, performance was worse than the default model (Fig. 7, top row). Similarly, model performance was worse when we constrained to large features (>250ms and >2 oct.), or removed all large features compared to the default model. When we constrained bandwidth and time independently to be large or small, model performance was worse compared to the default model, with large values being more detrimental (Fig. 7, bottom row). As previously discussed, using the largest possible features (whole calls or average call) resulted in poor classification performance as well. These results demonstrate that features of intermediate size indeed provide the best classification performance.

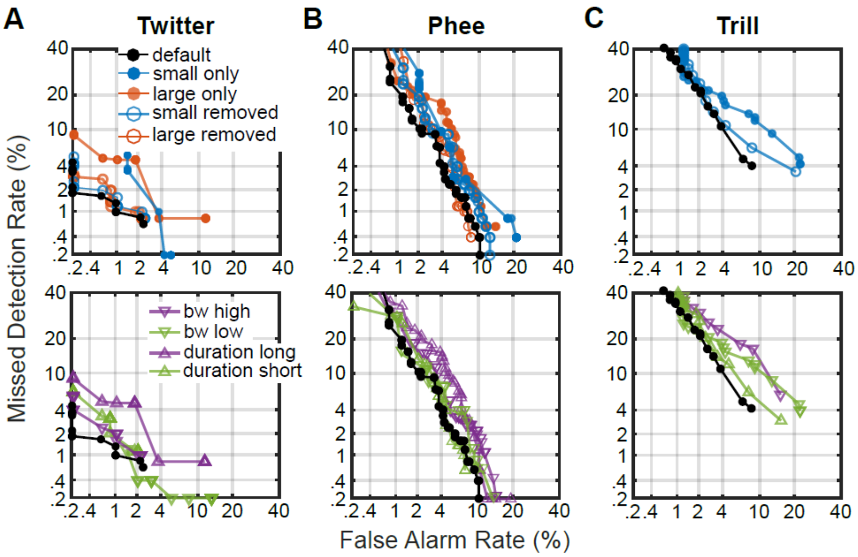

Figure 7: The precedence of intermediate features for classification. DET curves for call classification using features of different sizes, bandwidths, and durations for the classification of Twitters **(A)**, Phees **(B)**, and Trills **(C)**. In all these plots, the default model is in black. ***Top row*** shows performance when using small features only (<100 ms and <1 oct.) or excluding small features, and using large features only (>250 ms and >2 oct.) or excluding large features. For trills, some of these conditions fall outside the range of the axes. ***Bottom row*** shows performance when the bandwidth and duration of features used for classification were independently varied. Note that because of the short duration of trill calls, we did not test the effect of using only long duration features.

In this study, we used greedy search and pairwise maximization of information to find optimal features. However, it is possible that the greedy search algorithm does not find an optimal solution because of its inability to overcome local maxima. We do not think this is the case because: 1) the model performs at high accuracy levels, leaving little room for significant improvements, 2) we could arrive at similar sets of MIFs and achieve similar performance levels from different initial feature sets, specifically when highly informative features were excluded (Supp. Fig. 3), and 3) we could match or outperform other machine learning based algorithms for marmoset call classification[19]. Therefore, the implemented greedy search algorithm likely converges at a true optimal solution.

Factors contributing to the success of the MIF-based approach

Three factors were critical in the design and implementation of our approach. First, focusing on a behaviorally critical task (call categorization), and choosing model species with rich vocal repertoires and behaviors (marmosets and guinea pigs) allowed us to clearly identify a computational goal of cortical processing – call categorization. Previous experiments, both using electrophysiological[20 – 24] and imaging techniques[17, 25, 26], showing an increase in cortical resources allocated to call processing, validate our choice of call categorization as a critical computational goal in vocal animals. Second, our analyses were based on a large sample of calls recorded from a large number of animals[8]. From this data set, we deliberately oversampled a large number of initial potential features. This ensured that the full extent of production variability was represented in this data set. Third, the greedy search algorithm efficiently identified informative features from a training data set of a few hundred calls. Since clean and labelled training data sets are laborious to generate, the efficiency of greedy search provided a significant methodological advantage.

MIF-based reconstruction of call stimuli

The observation that an MIF-based approach successfully generalizes across production variability implies that most calls belonging to a category will contain one or more of the MIFs. Therefore, we asked how well calls could be reconstructed based on MIFs alone, using twitters as a specific example. To do so, we detected model twitter MIF neuron 'spiking' as earlier to the 500 training and 500 test twitters, and convolved these spike times with an alpha function (with a time constant of 20 ms) to detect the peak locations of twitter MIFs within a twitter (Supplementary Fig. 5A). We then placed copies of MIF cochleagrams at these peak locations, or added copies of MIF cochleagrams to previously placed feature cochleagrams. The final summed cochleagram was taken to be the reconstructed call (Supplementary Fig. 5B). We evaluated the accuracy of reconstruction as the NCC value at zero lag. The mean reconstruction accuracy was 0.69 (Supplementary Fig. 5C), suggesting that MIFs were indeed common denominators across twitter calls produced by different animals.

MIF tuning properties match some single unit recordings from A1 L2/3

So far, we have demonstrated that classification based on MIFs derived purely using theoretical principles can achieve high levels of production-invariant call categorization. We then asked if the auditory system uses such an optimal feature-based approach to call classification. To explore this possibility, as a first step, we generated 'tuning curves' of putative MIF-selective model neurons responding to commonly used acoustic stimuli and asked if these tuning curves matched previous experimental observations. In this effort, we were restricted by the appropriateness and availability of previous data. To do so, we first constructed cochleagrams of stimuli such as single and trains of frequency modulated sweeps, amplitude modulated tones, noise bursts, clicks, two-tone combinations, etc. We then used the maximum value of the NCC function as a metric of putative MIF neurons' 'response' to these stimuli, as we did earlier for test calls. These responses were conceptualized as 'membrane potential' responses, which elicited spiking only if they crossed each MIF neuron's optimal threshold. We used a power law nonlinearity, applied to the maximum NCC values (see Methods), to determine the firing rate responses of model MIF neurons (Supplementary Fig. 6). We then compared the MIF responses to available neural data from marmoset primary auditory cortex (A1).

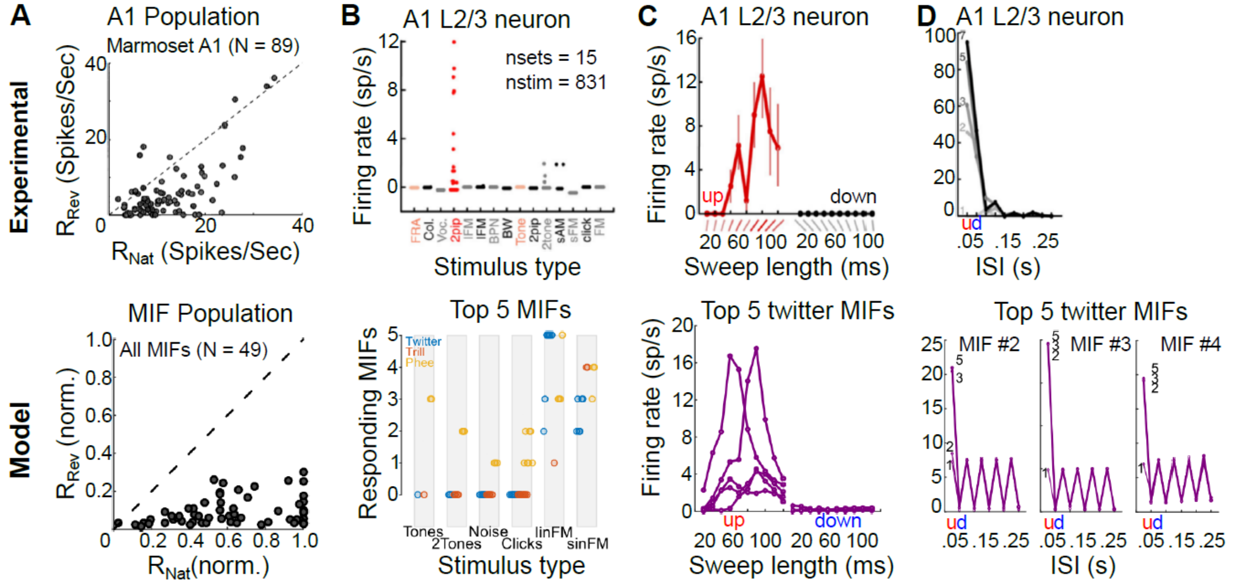

Figure 8: Predictions of putative MIF-neuron tuning properties match cortical data. (A – D, *top row*) Neural data from marmoset A1. **(A-D, *bottom row*)** Model predictions. **(A-*top*)** Preference of marmoset A1 responses for natural twitters over reversed twitters. **(A-*bottom*)** Preference of MIF neurons for natural calls over reversed calls. **(B-*top*)** Sparse responses of marmoset A1 L2/3 neuron. **(B-*bottom*)** Sparse responses of MIF neurons. The number of MIF neurons showing responses to the stimulus categories on the x-axis are plotted. Colors correspond to call type. **(C-*top*)** Marmoset A1 L2/3 neuron tuned to upward lFM sweeps of a specific length (~80 ms). **(C-*bottom*)** Twitter MIF neurons show similar tuning. **(D-*top*)** Marmoset A1 L2/3 neuron that does not respond to single lFM sweeps but shows tuning to trains of upward lFM sweeps with 50ms inter-sweep interval. Grayscale corresponds to the number of lFM sweeps in the train. **(D-*bottom*)** Three of the top 5 twitter MIFs showed similar tuning for lFM sweep trains. A-*top* reproduced from Wang and Kadia (2001), B-D *top* reproduced from Sadagopan and Wang (2009).

Although the MIF model was purely theoretical and did not have prior access to neurophysiological data, we found that model MIF neuron tuning recapitulated actual data to a remarkable degree, both at the population and single-unit levels. For example, the population of model MIFs showed high preference for natural calls compared to reversed calls (Fig.8A, bottom), similar to observations by Wang and Kadia[27] (reproduced in Fig. 8A, top). The high sparseness of auditory cortical neurons is welldocumented[28 – 30]. The responses of model MIF-selective neurons were also sparse – only few MIF neurons were activated by any given stimulus set, and only after extensively optimizing the parameters of the stimulus set to drive specific model MIF neurons. For example, in Fig. 8B (top), we show a single-unit recording from a marmoset A1 L2/3 neuron that did not respond to most stimulus types (reproduced from Sadagopan and Wang[30]), and only strongly responded to two-tone stimuli. Twitter MIFs (Fig. 8B, bottom) were similarly not responsive to most stimulus types, and only responded to carefully optimized linear frequency-modulated (lFM) sweeps. None of the model twitter and trill MIF-selective neurons responded to pure tones (Fig. 8B, bottom), similar to many A1 L2/3 neurons.

Most strikingly, we could recapitulate some specific and highly nonlinear single-neuron tuning properties as well. Figure 8C (top; reproduced from Sadagopan and Wang[30]) is a single-unit recording from marmoset A1 L2/3 that did not respond to pure tones, but selectively responded to upward lFM sweeps of specific lengths (~80 ms). Responses of at least three of the top 5 twitter MIF-selective model neurons showed similar tuning for 80 ms-long upward lFM sweeps (Fig. 8C, bottom). A second peak at ~40 ms was also present in responses of two model twitter MIF-selective neurons, also matching the experimental data. Figure 8D (top; reproduced from Sadagopan and Wang[30]) shows another single-unit recording from marmoset A1 L2/3, where the neuron did not respond to single lFM sweeps (lightest gray line), but strongly responded to trains of upward lFM sweeps occurring with 50 ms inter-sweep interval. The neuron's response scaled with the number of sweeps present in the train (darker colors correspond to more sweeps). Three of the top 5 twitter MIF-selective neurons also showed remarkably similar tuning (Fig. 8D, bottom). These model neurons did not respond to single sweeps as well, but responded to trains of at least 2 or more sweeps occurring with a 50 ms inter-sweep interval. Taken together, these data suggest neurons tuned to MIF-like features are present in A1 L2/3. Therefore, we would predict that a spectral-content based representation of calls in the ascending auditory pathway becomes largely a feature-based representation in A1 L2/3.

Consistent with the prediction of feature selectivity, we have found neurons in A1 of both marmosets and guinea pigs that respond selectively to conspecific call features. In Fig. 9, we present the spike rasters of example single neurons in both marmoset and guinea pig A1 responding to marmoset (Fig. 9A) and guinea pig calls (Fig. 9B) respectively. We presented multiple exemplars of each call type as stimuli. These example neurons responded at specific time points to a few call stimuli, typically across 1 – 3 categories. Such responses are consistent with our feature-based model because single features alone do not completely categorize calls, i.e., MIFs do not have 1 bit of information for categorization. Rather, combinations of features weighted by their log-likelihood ratios are necessary to ultimately achieve complete call category information. These data provide promising support for our model, but further experiments are necessary to: 1) determine how informative these neural features are about call category and how they compare with model features, 2) to confirm where such responses arise in the auditory pathway, and 3) to account for possible low-level confounds. Experiments are presently ongoing to address these issues.

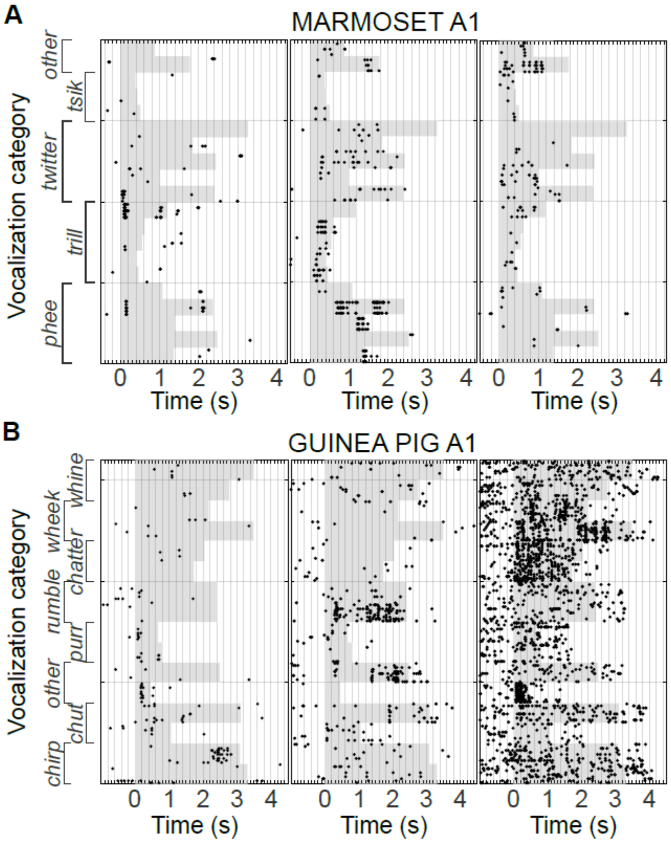

Figure 9: Feature selectivity in cortical neurons. (A) Spike rasters of three single units from marmoset A1 responding to marmoset call stimuli. Black dots correspond to spikes, gray shading corresponds to stimulus duration (different calls have different lengths). Note that spikes occur at specific times, and in response to 2 or 3 call types, suggesting that the neurons are responding to smaller features within these calls. **(B)** Spike rasters of three single units from guinea pig A1 responding to guinea pig call stimuli.

Task-dependent MIF-based classification as a general auditory computation

Our approach has two limitations. First, the number of auditory tasks that an animal is potentially required to solve is ill-defined. While we mitigate this limitation by choosing ethologically critical tasks such as call categorization, it is likely that we are only probing a small subset of all behaviorally relevant auditory tasks. Consequently, while a subset of neurons in auditory cortex match predictions from our model for call and caller classification, developing a larger bank of natural auditory behavior (for example, predator sounds versus neutral sounds) will allow us to model and predict a larger fraction of cortical responses. Second, our model derives features from the auditory nerve representation of stimuli. It is well-known that this representation is transformed more than once before impinging on cortical neurons. Therefore, the actual representation from which cortical neurons detect features are not accurately modeled here. This limitation arises from the current lack of predictive models for central auditory processing stages. It is possible that the performance of our algorithm will increase if we could accurately model other sub-cortical processing stages.

Recognizing these limitations, we asked if MIF-based representations of sounds could also be used for optimally solving other tasks, such as caller identification, and if MIF-based call classification also generalized to other vocal species. To test these hypotheses, we performed three proof-of-principle simulations using limited available data sets. For caller identification, we generated training and test sets of 60 twitters each from eight marmosets, and generated 500 initial random features from the training set. We applied the greedy-search algorithm to determine the MIFs for caller identification in a caller A vs. all other callers task (Fig. 10A). We found that similar to call categorization, caller identification could also be achieved using a small number of MIFs (n = 4). If caller identification was performed in a binary fashion (four classifications between two animals each), in half of these tasks, classification could be accomplished using less than 3 MIFs, indicating that the calls of these marmosets probably differed along the frequency axis. This is because if there are clear differences in dominant frequency (for example, Animal 1 vs. 4 in Fig. 1E), all features that Iie in one animal’s frequency range will detect all of that animal’s calls and none of the other animal’s calls. During the greedy search procedure, these features will be considered redundant and reduced to a single feature. In the other half, more MIFs were required for caller identification, and in general, MIFs were larger than those for call-type classification. This is likely because the differences between twitters produced by these animals are smaller compared to the differences between call types and can only be resolved in a higher dimensional space. Thus, integration over more frequencies and a larger time window may be necessary to resolve caller differences. In Supplementary Fig. 7, we plot the ROC for caller identification between a pair of marmosets with overlapping dominant frequencies. The MIF-based approach (n = 20 MIFs) achieved >80% hit rates with <10% false alarm rate for caller identification.

For determining the efficacy of MIF-based call classification in other species, we used guinea pig and macaque call classification as examples. Guinea pigs are highly vocal rodents that produce seven main call types[23, 31, 32], which are highly overlapping in the low frequency end of the spectrum, and show high production variability. We used the MIF-based approach to classify guinea pig call types (‘whine’, 'wheek', and ‘rumble’) from all other guinea pig call types. Similar to marmosets, guinea pig classification could be accomplished using a handful of features (12, 9, and 3 MIFs for whine, wheek, and rumble), and MIF-based classification achieved high performance levels (Fig. 10B). Similarly, we implemented the MIF-based algorithm to classify macaque calls (using 5, 4, and 9 MIFs for coos, grunts and harmonic arches) from a limited macaque call data set[33] and achieved high classification performance (Fig. 10C). These proof-of-principle experiments demonstrate that an MIF-based approach indeed succeeds for different auditory classification tasks and in different species, suggesting that building representations of sounds using task-relevant features in auditory cortex may be a general auditory computation.

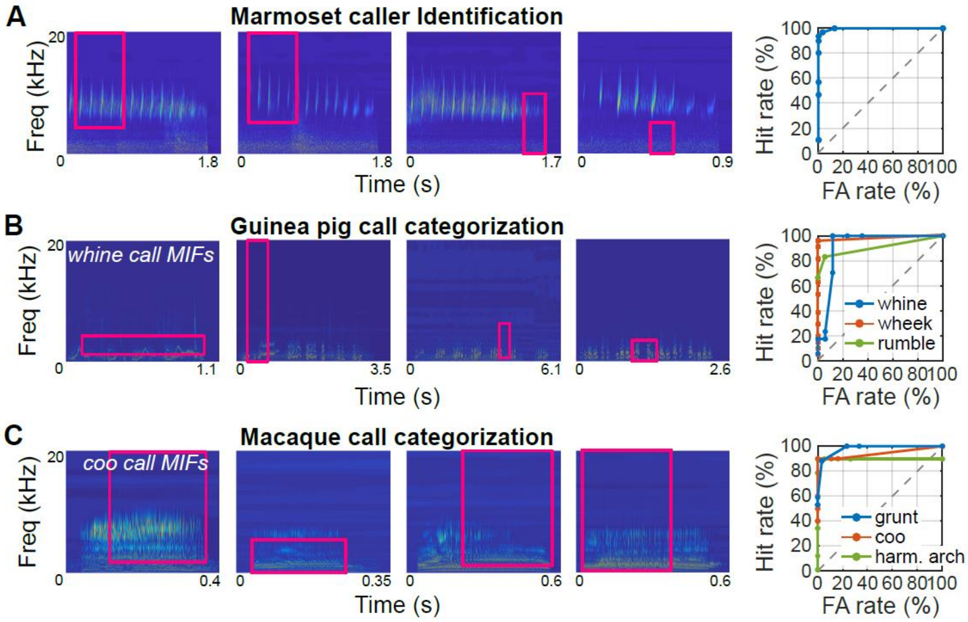

Figure 10: The applicability of MIF-based classification for other auditory tasks. The top four MIFs and ROC curves for: **(A)** marmoset caller identification (twitter calls), **(B)** Guinea pig call classification (MIFs for 'whine' calls shown), and **(C)** Macaque call classification (MIFs for 'coo' calls shown).

Discussion

In these experiments, we set out to understand the computations performed by the auditory system that enable the categorization of behaviorally critical sounds, such as calls, despite wide variations in the spectrotemporal structure of calls belonging to a category (production variability). We found that the optimal theoretical solution is to detect the presence of informative mid-level features (termed MIFs) in calls. These MIFs generalize over production variability, and conjunctions of MIFs accomplish production-invariant call classification with high accuracy. Critically, the tuning properties of putative MIF-selective neurons match previous recordings from marmoset A1 to a surprising degree. MIF-based classification was also successful for other tasks (marmoset caller identification), and in other species (guinea pig and macaque call recognition). Our results suggest that the representation of sounds in higher auditory cortical areas might enable performance of auditory tasks based on the detection of optimal task-relevant features.

Comparison to previous theoretical and experimental methods

An implication of our results is that in higher auditory processing stages, neural representations of sounds serve specific behavioral purposes. For example, the MIF-based classification approach that we proposed here is targeted to solve well-defined classification problems. At earlier stages of the auditory pathway, however, it may be more important to faithfully represent sounds using basis sets that enable the accurate encoding of novel stimuli. Previous theoretical studies have proposed, for example, that natural sounds can be efficiently encoded using spike patterns, where each spike represents the magnitude and timing of input acoustic features[34]. However, when optimized to encode the complete waveforms of natural sound ensembles, the kernel functions that elicit each spike show a striking similarity to cochlear filters. The advantage of this approach is that novel stimuli can be completely encoded using these kernel functions. In our approach, the input to our model implements a similar encoding schematic – in the cochleagram, inputs are encoded as spatiotemporal spike patterns, where each spike is the result of cochlear filtering. In this early representation, while information about category identity is present, it is distributed in the activity of many neurons in a high-dimensional space. We propose that in later processing stages, this early representation is transformed into a representation where category identity is more easily separable. By encoding MIF-like features, sound representation in later processing stages is less useful for high-fidelity encoding, but is instead goal-oriented. However, this means that each task will require a distinct set of MIFs for optimal performance, and animals likely perform a large number of such behaviorally relevant tasks. The observed 1000-fold increase between the number of cochlear inputs and auditory cortical neurons may partially result from this necessity to encode a multitude of task-dependent MIFs. Previous theoretical studies have suggested that the generation of redundant and over-complete representations of sounds to solve spatial localization problems might underlie this increase in the number of neurons[35]. Our study proposes another computational reason why such an expanded representation of sounds may be necessary.

A second class of increasingly popular models use hierarchical convolutional neural networks to accomplish classification tasks. In these models, layers of filtering, normalization and pooling operations are cascaded, resulting in individual units exhibiting increasingly complex tuning properties[36 – 38]. A final layer 'reads out' class identity. These ‘deep’ networks are a powerful set of models that claim to achieve near-human levels of performance on specific tasks, but carry some disadvantages. First, they often require training data of the order of millions of samples. In the visual domain, deep networks appear not to use the same features as humans for object classification[39]. Finally, an intuitive explanation for *how* deep network models actually accomplish classification is not available. In our approach, we explicitly train our MIF units to extract maximally distinguishing features, providing insight into *why* certain features are represented amongst these units. We consider our approach complementary to the deep learning approach, in that we aim to provide an explicit and intuitive explanation of why certain features are extracted, as opposed to matching human performance using complex model architectures.

Recently, theoretical efforts have been directed at learning invariant representations from small training sets using unsupervised methods[40]. In this model, image 'signatures' which serve as a proxy for the probability distribution of an image and its transformations are learnt by leveraging the time correlations of image transformations in the real world to label image identity. Image signatures can be computed by complex cell-like units using Hebbian learning rules. This model predicts that a similar computation might occur in auditory cortex. The MIFs that we have derived for call categorization are similar to the image 'signatures' in that they serve as a proxy for the probability distribution of a sound category that has been subjected to production variability. Indeed, vocalizations can be viewed as multivariate probability distributions along multiple call parameters[41], and MIFs could serve as the 'gist' of a call category around which these variations occur. Similar to image signatures, MIFs seem to be computed by superficial-layer auditory cortex neurons. However, differences arise in how MIFs are learnt. Although small sample sizes are adequate, unlike image 'signatures' that are learnt by observing image transformations over time, explicit labeling of the class of input examples is necessary for learning the MIFs of calls. Conceptually, whereas image 'signatures' are learnt by observing within-category transformations, MIFs are learnt by contrasting the distributions of sound categories.

Previous experimental studies have described call selectivity primarily using two methods: 1) categorization of neural tuning along an exhaustive list of call parameters[41], and 2) categorizing call tuning as tuning for regions of the modulation spectrum[42 – 44]. In the former study, marmoset calls were parametrized along multiple acoustic dimensions. Some of these parameters were common to all call types, such as the length or dominant frequency of a call. The more distinguishing parameters, however, were unique to individual call types, such as the inter-phrase interval for twitters, or sinusoidal frequency modulation rate for trills. Neural tuning to calls was described using tuning to these parameters but did not use the same set of parameters across call types. In our study, different MIFs are used for classification of different call types, but MIFs are parametrized along the same axes – bandwidth and integration window, allowing for a uniform basis for comparisons. In the latter set of studies, neural tuning for birdsong was described using selectivity for specific frequency and temporal modulations. In this case, tuning could be expressed in a unified stimulus space (of spectral- and temporal modulation rates). Both these methods, however, serve to *describe* neural tuning, and not to explain *why* tuning to certain parameters or regions of modulation space are necessary in the first place. Our results suggest that generating selectivity for task-relevant features explains why selectivity for stimulus parameters arises in the first place.

Possible mechanisms of generation of MIF-based representations

MIF-based representations are constructed from MIF-selective neurons. Neural selectivity for MIFs may be generated 1) gradually along the ascending auditory pathway, or 2) de-novo in cortex. Single-neuron feature selectivity often (but not always, see below) leads to selectivity for one or a few call types, and analyzing call selectivity of neurons at different auditory processing stages could provide insight into where MIF-based representations might be generated in the auditory pathway. In early auditory processing stages, evidence for call selectivity at the single-neuron level is minimal. For example, at the level of the cochlear nucleus, few single neurons in species other than mice show call selectivity[45]. At the level of inferior colliculus, a population-level bias in call-selectivity has been reported[45 – 47], but evidence for single-neuron level call-selectivity is equivocal[48]. It is only at the level of auditory cortex where clear single-neuron selectivity for calls or call features has been observed. Therefore, it is quite likely that selectivity for MIF-like features in species with spectrotemporally complex calls is generated at the level of auditory cortex. This is supported by the expansion in the number of cortical neurons mentioned above. Importantly, the cortical emergence of MIF-based representations is also supported by the fact that MIF-like responses have been observed in the superficial layers of marmoset A1[30].

We propose the following hierarchical model for auditory processing based on the representation of task-relevant features. In thalamorecipient layers of A1, representation of sound identity is still based on spectral content. This is reflected in the strongly tone-tuned responses of A1 L4 neurons. From these neurons, tuning for MIF-like features may be generated using nonlinear mechanisms such as combination-sensitivity. For example, the tuning properties of the marmoset A1 responses shown in Fig. 8 was determined to be the result of selectivity for precise spectral and temporal combinations of two tone pips[30]. This is also consistent with a recent computational model showing that combinations of spectrotemporal kernels, optimized for representing natural sounds, recreates aspects of experimentally observed spectrotemporal receptive fields from recordings in cat auditory cortex[49]. Further experiments, probing call and feature selectivity in identified layers of A1, are necessary to more precisely address where selectivity for MIF-like features first an emerges in the ascending auditory pathway.

The MIF-detection stage of processing is not necessarily categorically selective. In our model, the final decision about call category is the result of a weighted combination of MIF-detection responses. Since MIF-like features are likely represented in the superficial layers of A1, true call category selectivity likely arises in area further up the processing hierarchy. The most likely candidate for this read-out layer is the anterolateral belt region (AL) in primates[21], or the ventral-rostral belt (VRB) region in guinea pigs, where single-neurons have been shown to have high selectivity for call types[23]. We propose that belt neurons integrate a weighted combination of MIF-selective inputs to generate call category-selective responses. Weighted combination of synaptic inputs is a canonical neurophysiological operation, and our model does not involve any other specialized mechanisms.

What we have described are the emergent stages for the processing of behaviorally relevant sounds. Once categories are detected, further hierarchical processing stages might be necessary to accomplish more sophisticated behavioral goals such as caller identification[25], integration of social context with call perception, or decoding the emotional valence of calls.

Computations underlying the perception of auditory categories

In conclusion, we propose a hierarchical model for solving a central problem in auditory perception – the goal-oriented categorization of sounds that show high within-category variability such as speech[1, 2] or animal calls[3]. Our work has broad implications as to where in the auditory pathway categorization begins to emerge, and what features are optimal to learn in categorization tasks. For example, the lack of distinction of perceptual categories of English /r/ and /l/ by native Japanese speakers, and the success of bilingual Japanese speakers in accomplishing this classification, suggests that categorical differences can be learned[50]. Our model suggests that native speakers do not distinguish /r/-/l/ differences because the optimal features necessary for /r/-/l/ categorization are not encoded, as this categorization is not task-relevant for Japanese speech. FMRI evidence supports this conjecture[51]. Our model would predict that what is learned in bilingual speakers are optimal features that maximize /r/-/l/ differences. Our model would further predict that this learning would be primarily reflected in changes to the A1 L2/3 circuit. Consistent with this hypothesis, a recent study showed that training humans to categorize monkey calls resulted in finer tuning for call features in the auditory cortex[52]. We therefore suggest that the neural representation of sounds at higher cortical processing stages uses task-dependent features as building blocks, and that new blocks can be added to this representation to enable novel perceptual requirements.

Materials and Methods

Vocalizations: All procedures conformed to the NIH Guide for Care and Use of Laboratory Animals. All marmoset procedures were approved by the Institutional Animal Care and Use Committee (IACUC) of The Johns Hopkins University. All guinea pig procedures were approved by the IACUC of the University of Pittsburgh. We used vocalization recordings from 8 adult marmosets, both male and female, for these experiments. Marmoset calls were recorded from a marmoset colony at The Johns Hopkins University using directional microphones. Details of these recording techniques, and detailed characterizations of recorded calls are previously published[8]. Guinea pig calls were recorded from 3 male and 3 female adult guinea pigs. Two or more guinea pigs with varied social relationships were placed on either side of a transparent divider in a sound attenuated booth. Directional microphones, suspended above the guinea pigs were used to record calls. Calls were recorded using Sound Analysis Pro 2011[53], digitized at a sampling rate of 48 KHz, low-pass filtered at 24 KHz, manually segmented using Audacity, and classified into different call types.

Random feature generation: All modeling was implemented in MATLAB. We focused on classifying each of three major marmoset call types, *twitter*, *trill*, and *phee*, from all other call types. That is, three main binary classification tasks – *twitter* vs. all other calls, *trill* vs. all other calls, and *phee* vs. all other calls were considered. We set up the categorization tasks as a series of binary classifications (Twitter vs. all other calls, Trill vs. all other calls, etc.) based on the results of an earlier study of visual categorization that demonstrated the advantages of features learnt using multiple binary classifications compared to those learnt using a single multi-way classification. Specifically, in that study, multiple binary classifications resulted in features that were distinctive and highly tolerant to distortions[56]. For each classification task, we first generated training data sets, which consisted of 500 random within-class calls (e.g., *twitters*) produced by 8 animals (about 60 calls per animal), and 500 random outside-class calls (e.g., *trills*, *phees*, other calls) produced by the same 8 animals. In order to convert sound waveforms of the calls into a physiologically meaningful quantity, we transformed these calls into cochleagrams using a previously published auditory nerve model[54] using human auditory nerve parameters with high spontaneous rate. We used human auditory nerve parameters because of the close similarity between marmoset and human audiograms[55]. The output of this model was the time-varying activity pattern of the entire population of auditory nerve fibers, and resembles the spectrogram of the call (Fig. 2A, B). We then extracted 6000 random features from these 500 within-class cochleagrams. To do so, we randomly chose a center frequency, bandwidth, onset time and length and extracted a snippet of activity from the cochleagram. Each feature thus corresponded to the spatiotemporal pattern of activity of a subset of auditory nerve fibers within a specified time window (magenta box in Fig. 2B). We used rectangular feature shapes rather than other shapes to minimize assumptions – for example, an ellipse shaped feature would imply that the weighting of individual auditory nerve fibers changes over time. To ensure that smaller features were well-sampled, 2000 of these features were restricted to have a bandwidth less than 1 octave and a duration less than 100 ms. The bandwidth and duration of the remaining 4000 fragments were not constrained.

Threshold optimization: We defined the 'response' of a feature to a call as the maximum value of the normalized cross correlation (NCC) function between the feature's cochleagram and the call's cochleagram, restricted to the auditory nerve fibers that are represented in the feature. We effectively implemented a one-dimensional version of NCC by only considering the auditory nerve fibers that overlapped between the call and the feature. Note that this means features can only be detected in the frequency range that they span, but can be detected anywhere in time within a call. NCC is a commonly used metric to quantify template-match. To compute the NCC, the feature and the cochleagram patch at each lag were normalized by subtracting their respective mean values and dividing by their respective standard deviations before convolving them. This results in a value between -1, signifying that the feature and cochleagram patch at that lag are completely anti-correlated, and +1, signifying a perfect match between the feature and the cochleagram. Because this is a computation-intensive step, template matching was implemented on an NVIDIA GeForce 980 Ti GPU. For each feature, then, we obtained 500 within-class responses, and 500 outside-class responses (response histograms of an example feature in Fig. 2C). To transform these continuous response distributions into a binary detection variable, we used mutual information to quantify the information provided by a feature about the class (within- or outside-class) over a parametrically varied range of thresholds. We computed mutual information following the method of Ullman et al.[12], by measuring the frequency of detecting a feature f_i at a given threshold θ_i (f_i = 1 if present, 0 if absent) in the within-class (C=1) or outside-class (C=0) cochleagrams as:

$$I(f_i(\theta_i), C) = \sum_{\substack{f_i = \{0,1\} \\ C = \{0,1\}}} p(f_i, C) \log\left(\frac{p(f_i, C)}{p(f_i)p(C)}\right)$$

where P(C) was assumed to be 0.10. We empirically verified that features identified were insensitive to variations of this value. The optimal threshold for each feature was taken to be the threshold value at which the mutual information was maximal, and the merit of each feature was taken to be the maximum mutual information value in bits (Fig. 2C). The 'weight' of each feature was taken to be its log-likelihood ratio. At the end of this procedure, each of the initial 6000 features were allocated a merit, a weight, and an optimal threshold at which each individual feature's utility for classifying calls as belonging to within- or outside-class was maximized. Note that merit and weight are distinct quantities that need not be monotonically related. For example, if the *lack* of energy in a frequency band is indicative of a target category, features that contain energy in this frequency band will be detected often in the other categories, but not in the target category. The feature will thus have high merit for classification, as it is informative by its absence, but have a negative weight.

Greedy search: Because we chose initial features are random, many of these features individually provided low information about call category, and many of the best features for classification were self-similar, or redundant. Therefore, to extract maximal information from a minimal set of features for classification, we used a greedy search algorithm[12] to iteratively 1) eliminate redundant features, and 2) pick features that add the most information to the set of selected features. The minimal set of features that together maximize information about call type were termed maximally informative features (MIFs). The first MIF was chosen to be the feature with maximal merit from the set of all 6000 initial random features. Every consecutive MIF was chosen to maximize pairwise added information with respect to the previously chosen MIFs. Note that these consecutive features need not have high merit individually. We iteratively added MIFs until we could no longer increase the hit rate without increasing the false alarm rate. Practically, this meant adding features until total information reached 0.999 bits, or individual features added less than 0.001 bits, whichever was reached earlier. At the end of this procedure, a small set of MIFs, containing the optimal set of features for call classification was obtained.

Analysis and statistics: To test how well novel calls could be classified using these MIFs alone, we generated from the same 8 animals a test set of 500 within- and outside-class calls that the model had not been exposed to before. We computed the NCC between each test call and MIF, and considered the MIF to be detected in the call if the maximum value of the NCC function exceeded its optimal threshold. If detected, the MIF provided evidence in favor of a test call belonging to a call type, proportional to its log-likelihood ratio. We then summed the evidence provided by all MIFs and generated ROC curves of classification performance by systematically varying an overall evidence threshold. We used the area under the curve (AUC) to compare ROC curves for classification performance by MIFs generated with different constraints (see Results). Statistical significance was evaluated using non-parametric methods for comparing between these conditions, and for comparing performance to a large number of simulations generated using random MIFs.

Generating predictions: To generate predictions of the 'responses' of putative MIF-selective neurons to other auditory stimuli, we first generated a large battery of stimuli encompassing stimuli used in previous recordings from marmoset A1 in MATLAB and computed their cochleagrams as earlier. We then computed the maximum value of the NCC function between the MIF and the stimulus cochleagram. This resulted in response values that could be conceptualized as equivalent to membrane potential (V_m) responses. These were converted to firing rates by applying a power law nonlinearity, of the form:

$$FR = k \, . \, [V_m - \theta]^p$$

Where FR is the firing rate response in spk/s, θ is the MIF's optimal threshold, p is the exponential nonlinearity set to a value of 4, and k is an arbitrary scaling factor.

Call reconstruction from MIFs: To reconstruct calls, we conceptualized MIFs as MIF-selective neurons, and considered the times at which NCC values exceeded the optimal threshold to be the spike times of these neurons. MIF spike times were computed with a time resolution of 2 ms to simulate refractoriness, and alpha-functions were convolved with the spike times to determine the peak time at which each MIF was detected. A copy of the MIF cochleagram was then placed at the peak time, or summed (with log-likelihood weights) if overlapping with a previously placed cochleagram. The accuracy of reconstruction was defined as the NCC between the original stimulus and its reconstructed version at zero lag.

Electrophysiology methods: Predictions generated from the MIFs were compared to earlier recordings from marmoset A1. Details of recording procedures are available from original experimental data sources. All recordings were from adult marmosets. Population data comparing natural to reversed twitters were obtained from Wang and Kadia[27]. These experiments were performed in anesthetized marmosets. Single-neuron data regarding feature selectivity were obtained from Sadagopan and Wang[30]. These recordings were from awake, passively-listening marmosets. Single-neuron data regarding feature selectivity in guinea pigs were obtained from adult, head-fixed, passively-listening guinea pigs at the University of Pittsburgh. Briefly, a headpost and recording chambers were secured to the skull using dental cement following aseptic procedures. Animals were placed in a double-walled, anechoic, sound attenuated booth. A small craniotomy was performed over auditory cortex. High-impedance tungsten electrodes (3 – 5 MΩ, A-M Systems Inc. or FHC, Inc.) were advanced through the dura into cortex to record neural activity. Stimuli were generated in MATLAB, and presented (TDT Inc.) from the best location in an azimuthal speaker array (B&W-600S3 or Fostex FT-28D for marmosets, TangBand 4” full-range driver for guinea pigs). Single units were sorted online using a template matching algorithm (Alpha Omega Inc. or Ripple, Inc), and for guinea pigs, refined offline (MKSort). All analyses were performed using custom MATLAB code.

Code availability: Custom code will be provided upon request to the corresponding author (SS).

References

1. Peterson GE, Barney HL (1952) Control methods used in a study of the vowels. J Acoust Soc Am 24:175–184.
2. Hillenbrand J, Getty LA, Clark MJ, Wheeler K (1995) Acoustic characteristics of American English vowels. J Acoust Soc Am 97:3099-111.
3. Wang X (2000). On cortical coding of vocal communication sounds in primates PNAS 97:11843-11849.
4. Epple G (1968) Comparative studies on vocalization in marmoset monkeys (hapalidae). Folia Primatol. 8:1–40.
5. Chen HC, Kaplan G, Rogers LJ (2009) Contact calls of common marmosets (Callithrix jacchus): influence of age of caller on antiphonal calling and other vocal responses. AM J Primatol 71:165-170.
6. Miller CT, Mandel K, Wang X (2010) The communicative content of the common marmoset phee call during antiphonal calling. AM J Primatol 72:974–980.
7. Kato Y, Gokan H, Oh-Nishi A, Suhara T, Watanabe S, Minamimoto T (2014) Vocalizations associated with anxiety and fear in the common marmoset (Callithrix jacchus). Behav Brain Res 2275:43-52.
8. Agamaite JA, Chang C-J, Osmanski MS, Wang X (2015) A quantitative acoustic analysis of the vocal repertoire of the common marmoset (Callithrix jacchus). J Acoust Soc Am 138:2906–2928.
9. Tsao DY, Livingstone MS (2008) Mechanisms of face perception. Annu Rev Neurosci 31:411–437.
10. Jenkins R, White D, Van Montfort X, Mike Burton A (2011) Variability in photos of the same face. Cognition 121:313-323.

11. Kramer RSS, Manesi Z, Towler A, Reynolds MG, Burton AM (2018) Familiarity and Within-Person Facial Variability: The Importance of the Internal and External Features. Perception 47:3-15.

12. Ullman S, Vidal-Naguet M, Sali E (2002) Visual features of intermediate complexity and their use in classification. Nat Neurosci. 5:682-687.

13. Viola P, Jones M (2004). Robust real-time face detection. International journal of computer vision 57:137-154.

14. Sinha P (2002) Qualitative representations for recognition. Proceedings of the Annual Workshop on Biologically Motivated Computer Vision. 249–262.

15. Lerner Y, Epshtein B, Ullman S, Malach R(2008) Class information predicts activation by object fragments in human object areas. J Cogn Neurosci 20:1189-1206.

16. Issa EB, DiCarlo JJ (2012) Precedence of the eye region in neural processing of faces. J Neurosci 32:16666-16682.

17. Sadagopan S, Temiz-Karayol NZ, Voss HU (2015) High-field functional magnetic resonance imaging of vocalization processing in marmosets. Sci Rep 5:10950.

18. Ullman S, Bart E (2004) Recognition invariance obtained by extended and invariant features. Neural Netw 17:833-848.

19. Turesson HK, Ribeiro S, Pereira DR, Papa JP, de Albuquerque VHC (2016). Machine learning algorithms for automatic classification of marmoset vocalizations. PLoS One 11: e0163041.

20. Rauschecker JP, Tian B (2000) Mechanisms and streams for processing of "what" and "where" in auditory cortex. Proc Natl Acad Sci USA 97:11800-11806.

21. Tian B, Reser, D, Durham A, Kustov A, Rauschecker JP (2001) Functional Specialization in Rhesus Monkey Auditory Cortex. Science 292:290-293.
22. Romanski LM, Averbeck BB (2009) The primate cortical auditory system and neural representation of conspecific vocalizations. Annu Rev Neurosci. 32:315-346.
23. Grimsley JM, Shanbhag SJ, Palmer AR, Wallace MN (2012) Processing of communication calls in guinea pig auditory cortex. PLoS One 7:e51646.
24. Fukushima M, Saunders RC, Leopold DA, Mishkin M, Averbeck BB (2014) Differential coding of conspecific vocalizations in the ventral auditory cortical stream. J Neurosci 26:4665-4676.
25. Petkov CI, Kayser C, Steudel T, Whittingstall K, Augath M, Logothetis NK (2008) A voice region in the monkey brain. Nat Neurosci 11:367-374.
26. Perrodin C, Kayser C, Logothetis NK, Petkov CI (2011) Voice cells in the primate temporal lobe. Curr Biol 21:1408-1415.
27. Wang X, Kadia SC (2001) Differential representation of species-specific primate vocalizations in the auditory cortices of marmoset and cat. J Neurophysiol 86:2616-2620.
28. Hromádka T, Deweese MR, Zador AM (2008) Sparse representation of sounds in the unanesthetized auditory cortex. PLoS Biol 6: e16.
29. Hromádka T, Zador AM (2009) Representations in auditory cortex. Curr Opin Neurobiol 19:430-433.
30. Sadagopan S, Wang X (2009) Nonlinear spectrotemporal interactions underlying selectivity for complex sounds in auditory cortex. J Neurosci 29:11192-11202.

31. Eisenberg JF (1974) The function and motivational basis of hystricomorph vocalizations. Symp Zool Soc Lond 34: 211–247.

32. Berryman JC (1976) Guinea-pig vocalizations: their structure, causation and function. Z Tierpsychol 41:80-106.

33. Hauser MD (1998) Functional referents and acoustic similarity: field playback experiments with rhesus monkeys. Anim Behav 55: 1647 – 1658.

34. Smith EC, Lewicki MS (2006) Efficient auditory coding. Nature 439:978-982.

35. Asari H, Pearlmutter BA, Zador AM (2006) Sparse representations for the cocktail party problem. J Neurosci 26:7477-7490.

36. Räsänen O, Nagamine T, Mesgarani N (2016) Analyzing Distributional Learning of Phonemic Categories in Unsupervised Deep Neural Networks. Cogsci 2016:1757-1762.

37. Khalighinejad B, Cruzatto da Silva G, Mesgarani N (2017) Dynamic Encoding of Acoustic Features in Neural Responses to Continuous Speech. J Neurosci 37:2176-2185.

38. Kell AJE, Yamins DLK, Shook EN, Norman-Hagniere SV, McDermott JH (2018) A task optimized neural network replicates human auditory behavior, predicts brain responses, and reveals a cortical processing hierarchy. Neuron 98: 630 – 644.

39. Ullman S, Assif L, Fetaya E, Harari D (2016) Atoms of recognition in human and computer vision. Proc Natl Acad Sci USA 113: 2744 – 2749.

40. Anselmi F, Leibo JZ, Rosasco L, Mutch J, Tacchetti A, Poggio T (2016) Unsupervised learning of invariant representations. Theor Comput Sci 633: 112 – 121.

41. DiMattina C, Wang X (2006) Virtual vocalization stimuli for investigating neural representations of species-specific vocalizations. J Neurophysiol 95:1244-1262.

42. Hsu A, Woolley SM, Fremouw TE, Theunissen FE. (2004) Modulation power and phase spectrum of natural sounds enhance neural encoding performed by single auditory neurons. J Neurosci. 24:9201-9211.

43. Woolley SM, Fremouw TE, Hsu A, Theunissen FE (2005) Tuning for spectro-temporal modulations as a mechanism for auditory discrimination of natural sounds. Nat Neurosci 8:1371-1379.

44. Stowell D, Plumbley MD (2014) Large-scale analysis of frequency modulation in birdsong data bases. Methods in Ecology and Evolution 5:901-912.

45. Pollak GD (2013) The dominant role of inhibition in creating response selectivities for communication calls in the brainstem auditory system. Hear Res 305:86-101.

46. Portfors CV, Roberts PD, Jonson K (2009) Over-representation of species-specific vocalizations in the awake mouse inferior colliculus. Neuroscience 18:486-500.

47. Holmstrom LA, Eeuwes LB, Roberts PD, Portfors CV (2010) Efficient encoding of vocalizations in the auditory midbrain. J Neurosci 30:802-819.

48. Suta D, Kvasnák E, Popelár J, Syka J (2003) Representation of species-specific vocalizations in the inferior colliculus of the guinea pig. J Neurophysiol 90:3794-3808.

49. Mlynarski W, McDermott JH (2017) Learning midlevel auditory codes from natural sound statistics. Neural Comput 8:1-39.

50. MacKain KS, Best CT, Srange W (1981) Categorical perception of English /r/ and /l/ by Japanese bilinguals. Applied Psycholinguistics 2:369-390.

51. Raizada RDS, Tsao F, Liu H, Kuhl PK (2010) Quantifying the Adequacy of Neural Representations for a Cross-Language Phonetic Discrimination Task: Prediction of Individual Differences. Cereb Cortex 20:1-12.

52. Jiang X, Chevillet MA, Rauschecker JP, Riesenhuber M (2018) Training humans to categorize monkey calls: auditory feature- and category-selective neural tuning changes. Neuron 98: 405 – 416.

53. Tchernichovski O, Nottebohm F, Ho CE, Pesaran B, Miltra PP (2000) A procedure for an automated measurement of song similarity. Anim Behav 59:1167-1176.

54. Zilany MS, Bruce IC, Carney LH (2014) Updated parameters and expanded simulation options for a model of the auditory periphery. J. Acoust. Soc. Am.126:2390–2412.

55. Osmanski MS, Wang X (2011) Measurement of absolute auditory thresholds in the common marmoset (Callithrix jacchus). Hear Res 277: 127 – 33.

56. Akselrod-Ballin A, Ullman S (2008) Distinctive and compact features. Image and Vision Computing, 26:1269-1276.

Acknowledgements

We thank Dr. Yale E. Cohen for generously providing us with a set of macaque vocalizations. Patrick Haggerty and Vighnesh Viswanathan contributed some of the analysis in this paper. Samuel Li and Isha Kumbam assisted in the recording and curation of guinea pig vocalizations. SS was supported with funding from the NIH (NIDCD R01DC017141), the Departments of Otolaryngology and Neurobiology, the Pennsylvania Lions Hearing Research Foundation, and the Samuel and Emma Winters foundation. STL was supported by a T-32 Training grant in Auditory and Vestibular Neuroscience (NIDCD T32DC011499).

Author Contributions

SS designed and implemented an initial version of the model with advice and vocalization data provided by XW. STL and SS were responsible for all subsequent model development and comparisons of the model to data. PML collected and analyzed neural data from guinea pig auditory cortex, and recorded and categorized guinea pig vocalizations. STL and SS co-wrote the manuscript with inputs from XW.

Competing interests

The authors declare no competing financial interests.

Materials and Correspondence

Requests for materials and correspondence to SS (vatsun@pitt.edu).

Supplementary Material

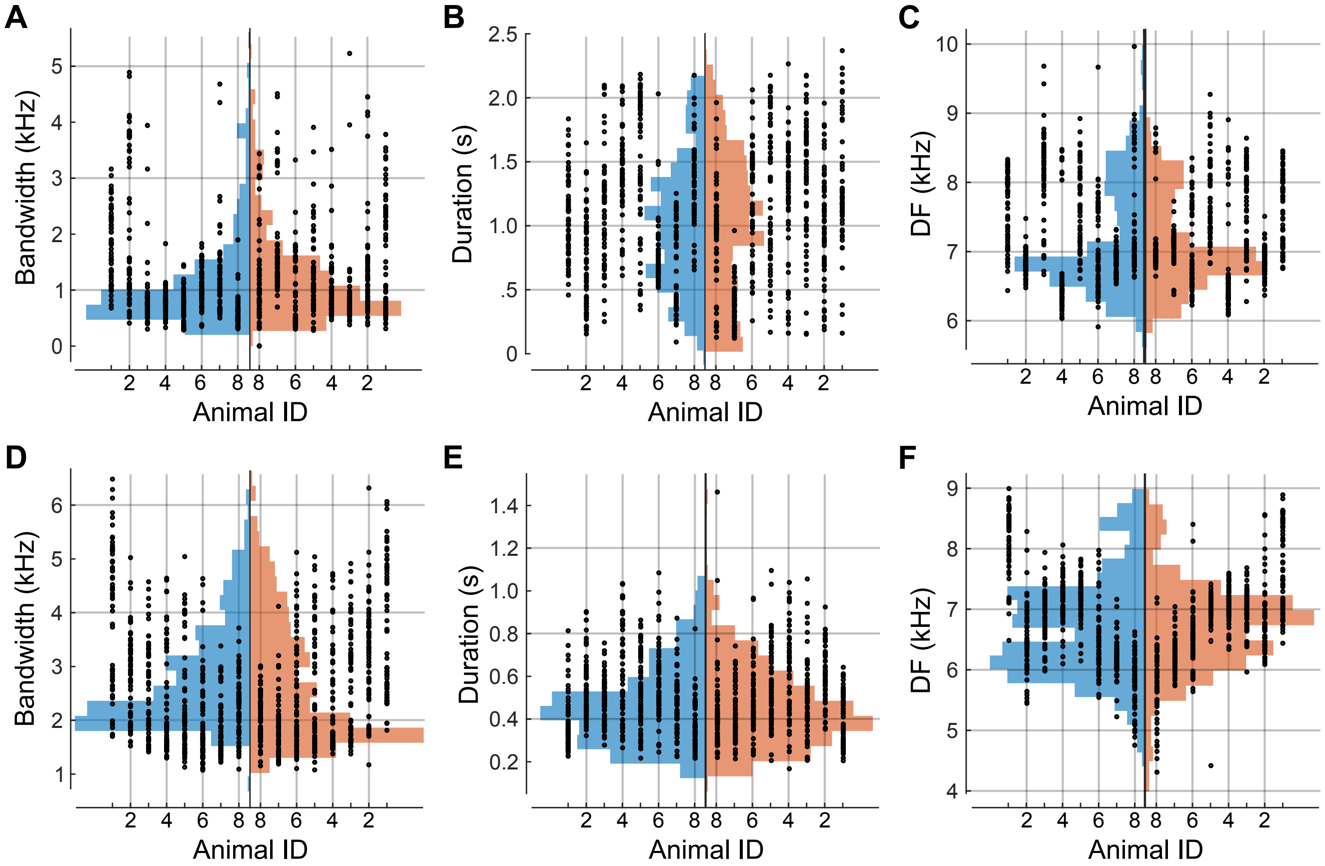

Supplementary Figure 1: Production variability of major marmoset call types. (A-C) Production variability of phee calls quantified along various parameters: **(A)** bandwidth, **(B)** duration, and **(C)** dominant frequency. Dots depict parameter values for single calls, and histograms indicate the overall distribution of these parameters, split into the training (blue) and testing (red) sets. **(D-F)** Production variability of trill calls quantified as in (A-C).

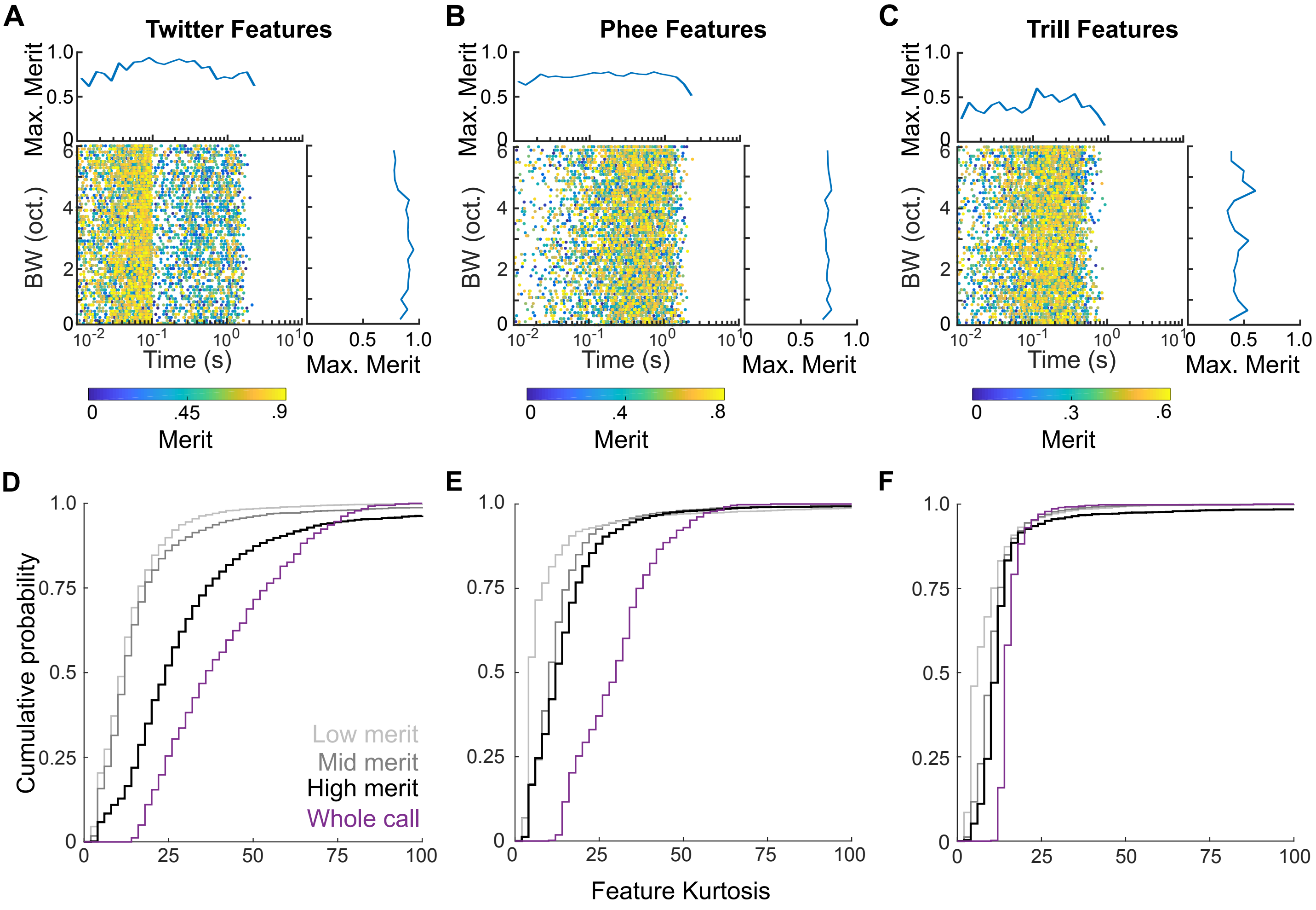

Supplementary Figure 2: Information content, complexity, and size of all initial random features. Scatter plot of all 6000 features generated for each call type: twitter **(A)**, phee **(B)**, and trill **(C)**, as a function of their bandwidth and temporal extent. Color scale corresponds to the merit of each feature. Marginal histograms depict the maximum merit in each time- or bandwidth-bin. **(D-F)** Features of high merit for classifcation tend to be of intermediate complexity. Merit vs complexity plot of all randomly generated twitter **(D)**, phee **(E)**, and trill **(F)** features. Feature complexity is estimated to be proportional to the reduced kurtosis of the distribution of activity within a feature or call. In these plots, low- or mid-merit features (defined as the bottom 33-%ile (light gray) and 33rd - 66th %-ile (dark gray)) show distributions of low kurtosis values. Whole calls show high kurtosis values (purple). Across call types, high-merit features (top 33%-ile) show intermediate kurtosis values, indicating that high-merit features are of intermediate complexity.

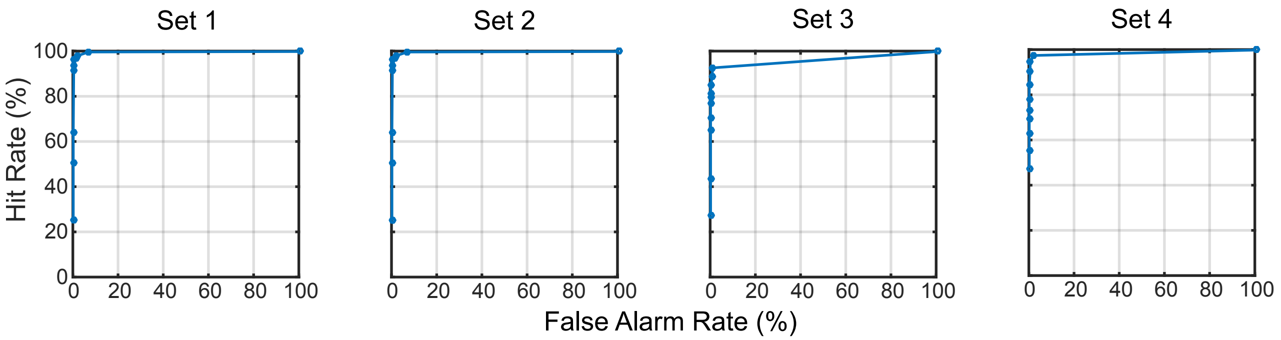

Supplementary Figure 3: Similar classification performance obtained using distinct MIF sets. ROC curves for twitter classification using four successive iterations of MIFs, generated by removing all MIFs from the previous set, and selecting MIFs from the remaining features. High performance demonstrates that feature space was adequately sampled, and that the algorithm was not stuck in local maxima.

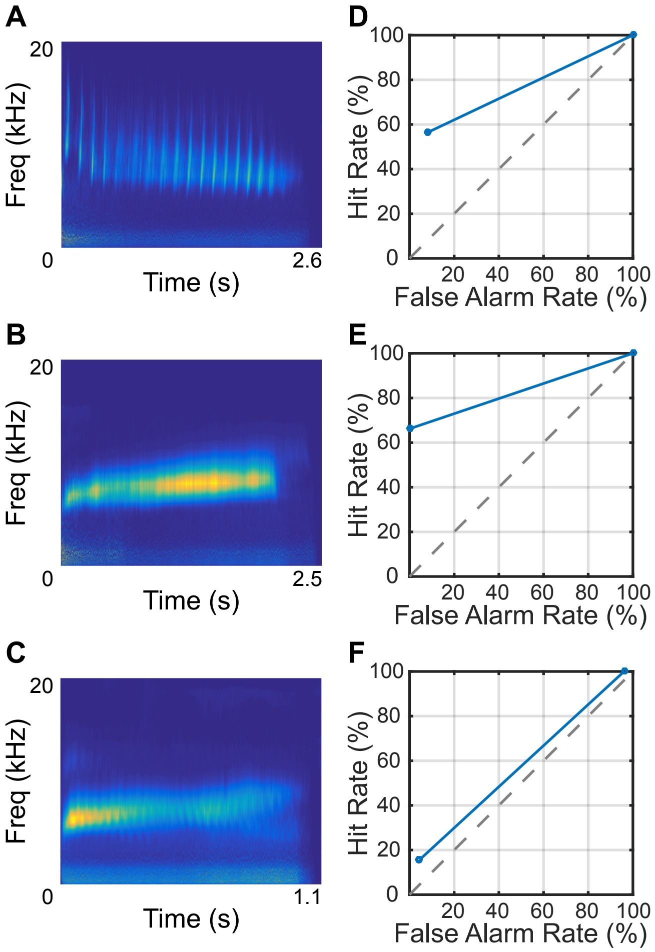

Supplementary Figure 4: Classification using average calls. An average twitter **(A)**, trill **(B)**, and phee **(C)** constructed by aligning and averaging over the calls. **(D-F)** Classification performance using the average call as the single informative feature.

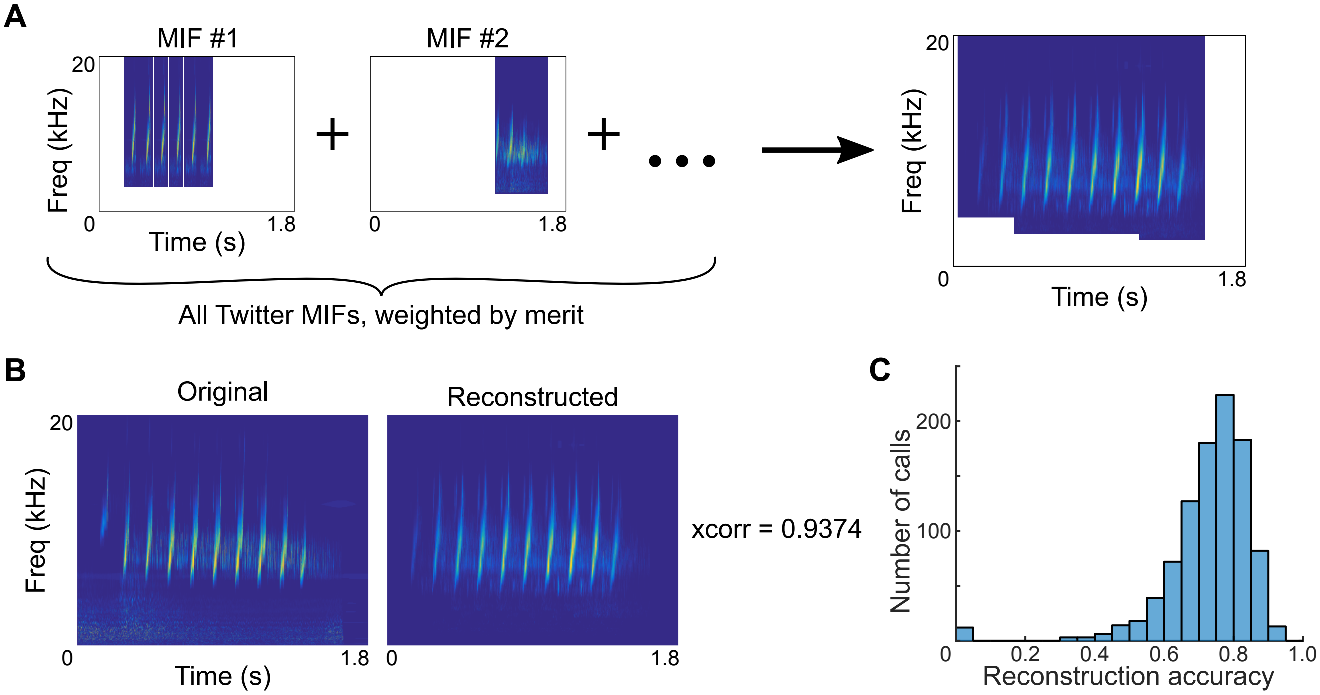

Supplementary Figure 5: Reconstruction of twitter calls using only twitter MIFs. (A) Cochleagrams of MIFs were placed at the time points at which MIFs were detected within a sample twitter call. All MIF cochleagrams were then summed, weighted by their log-likelihood ratios. **(B)** Cochleagrams of and example original twitter call and its reconstructed version. **(C)** Histogram of the reconstruction accuracy of 1000 twitter calls.

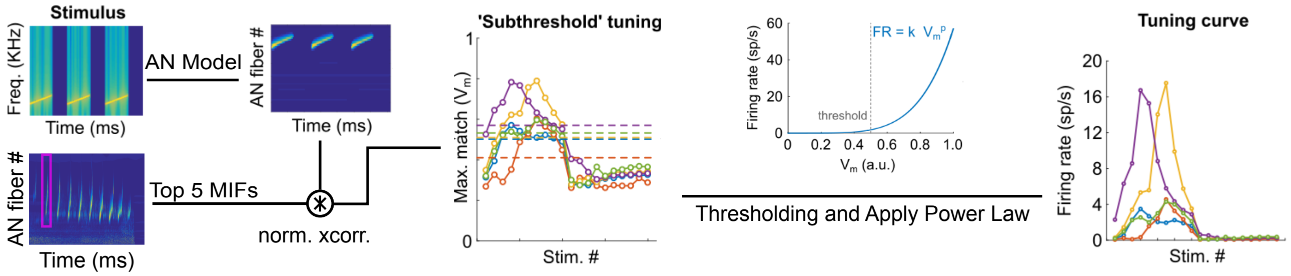

Supplementary Figure 6: Simulation of putative MIF-neuron tuning properties. The responses of MIFs to cochleagrams of commonly used auditory stimuli were taken to be the maximum value of the normalized cross-correlation function. A power law nonlinearity was applied to this value to obtain 'tuning curves' of the MIF-neurons to these stimuli.

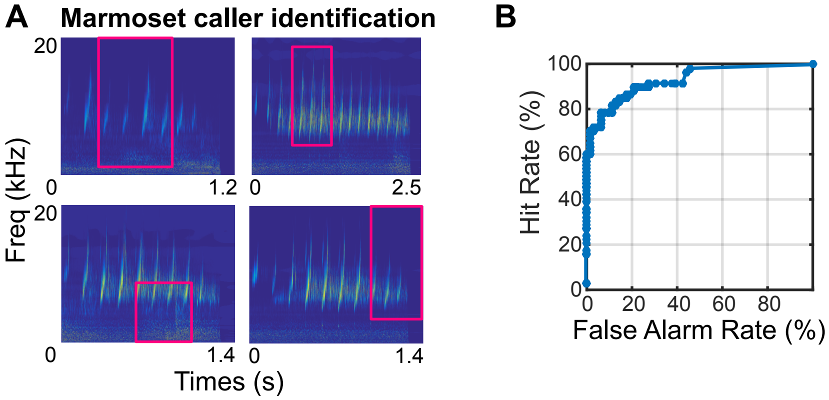

Supplementary Figure 7: Caller identification for a pair of marmoset callers with overlapping dominant frequencies. (A) MIFs for caller identification. **(B)** ROC curve for caller identification.